Synthesis of Remote Sensing Label Fields Using a Tree-Structured Hierarchical Model

Ying Liu, *Student Member, IEEE*, Alexander Wong, *Member, IEEE*, and Paul Fieguth, *Member, IEEE*

***Abstract*—The systematic evaluation of synthetic aperture radar (SAR) data analysis tools, such as segmentation and classification algorithms for geographic information systems, is difficult given the unavailability of ground-truth data in most cases. Therefore, testing is typically limited to small sets of pseudo-ground-truth data collected manually by trained experts, or primitive synthetic sets composed of simple geometries. To address this issue, we investigate the potential of employing an alternative approach, which involves the synthesis of SAR data and corresponding label fields from real SAR data for use as a reliable evaluation testbed. Given the scale-dependent nonstationary nature of SAR data, a new modeling approach that combines a resolution-oriented hierarchical method with a region-oriented binary tree structure is introduced to synthesize such complex data in a realistic manner. Experimental results using operational RADARSAT SAR sea-ice data and SIR-C/X-SAR land-mass data show that the proposed hierarchical approach can better model complex nonstationary scale structures than local MRF approaches and existing nonparametric methods, thus making it well suited for synthesizing SAR data and the corresponding label fields for potential use in the systematic evaluation of SAR data analysis tools.**

***Index Terms*—Data synthesis, hierarchical, Markov random field (MRF), remote sensing, sea ice, synthetic aperture radar (SAR).**

I. Introduction

THE USE of aerial and satellite remote sensing data has become an integral part of terrestrial ecological studies and environmental monitoring, ranging from sea-ice monitoring in polar regions [1] and land-use and land-cover change analysis [2], [3] to flood risk and damage assessment [4]. Given the large volume of high-resolution remote sensing data being acquired on a daily basis and the time-consuming nature of manual data manipulation, considerable research effort in the design of geoscience information systems (GIS) has been spent on the development of tools for analyzing remote sensing data in an automated fashion. Two classes of automatic data analysis tools that have great importance to GIS are automatic segmentation [1], [5]–[8] and classification algorithms [4], [9]–[12].

A major challenge in the design of automatic segmentation and classification algorithms for the purpose of remote sensing data analysis is the reliable systematic evaluation of algorithmic performance. While a plethora of quantitative assessment metrics are available for evaluating the performance of such automatic data analysis tools [13], it is very difficult, even intractable in the case of synthetic aperture radar (SAR) data analysis of polar regions and mountainous land-mass regions, to acquire ground-truth segmentation and classification information pertaining to the data. As such, the evaluation of automatic segmentation and classification techniques has been limited to the use of small sets of pseudo-ground-truth data collected manually by trained experts in a time-consuming manner, or primitive synthetic sets composed of simple geometric shapes [1]. The reliability of performance assessment using pseudo-ground-truth data is limited not only by the small set of test data available but also by the limited time and accuracy of trained experts who are able to produce manual segmentations and classifications on a per-sample level. The performance assessment using primitive synthetic sets is more reliable than that using pseudo-ground-truth data given the large amount of test data available and per-sample level accurate ground truth. However, such primitive synthetic tests are a poor representation of real remote sensing data and, as such, do not provide a realistic testing scenario for evaluating the operational potential of an automatic data analysis algorithm.

To address these issues associated with the evaluation of automatic analysis algorithms, we investigate the potential of synthesizing realistic looking data, based on models trained from real data, but with corresponding synthesized ground-truth label fields. This approach allows for the generation of large test sets that are representative of real-world operational scenarios and have *known* ground truth. Furthermore, the randomness associated with the synthesis process improves the reliability of testing by reducing bias toward algorithms tuned to work well with specific test data.

There is a significant research literature in remote sensing dealing with model-based texture synthesis [14]–[17]. However, such methods are designed to capture and generate textural characteristics only and, as such, are ill suited for generating realistic looking remote sensing data as they do not capture the complex structural characteristics found in operational settings. More recent general nonparametric texture synthesis methods (e.g., [18]–[20]) are able to better capture both textural and structural characteristics but exhibit two main limitations. First, they are ill suited for capturing large-scale structural characteristics, which will be illustrated later in the experimental results and, second, they do not provide a corresponding label field which is the necessary ground truth in evaluation.

One region-based posterior sampling method has been recently proposed [21], which simultaneously samples the data and corresponding label field for SAR data. While more

Manuscript received October 11, 2009; revised March 25, 2010 and August 3, 2010; accepted November 28, 2010. Date of publication February 6, 2011; date of current version May 20, 2011.

The authors are with the Department of Systems Design Engineering, University of Waterloo, Waterloo, ON N2L 3G1, Canada (e-mail: y30liu@uwaterloo.ca; a28wong@uwaterloo.ca; pfieguth@uwaterloo.ca).

Color versions of one or more of the figures in this paper are available online at http://ieeexplore.ieee.org.

Digital Object Identifier 10.1109/TGRS.2010.2102765

suitable as an evaluation testbed, this approach shares similar limitations to other patch-based nonparametric methods (e.g., [19], [20]) in terms of sensitivity to patch size. Moreover, the method of [21] emphasizes SAR texture as opposed to the ground-truth label field, so the synthesized label fields suffer from artifacts, as will be seen in the experimental results.

In this paper, we aim to address the issues faced by existing synthesis methods in generating realistic-looking SAR data by decoupling the synthesis of texture and structure. That is, we will *explicitly* synthesize the discrete-state label field, which contains the complex structural characteristics of the problem, and separately synthesize the textural characteristics of the data using a modification of the nonparametric texture synthesis strategy proposed by Efros and Leung [18]. We introduce a practical approach to synthesizing multilabel discrete fields by combining a resolution-oriented hierarchy with a region-oriented hierarchy [22]–[24]. Indeed, recently, there has been a growing interest in the generalization of hierarchical partition fields [25], [26] for the segmentation of hidden hierarchical fields [27]; however, the idea of using partition trees and hierarchical models for data synthesis is novel.

This paper is organized as follows. Research literature related to data synthesis is discussed in Section II. The underlying theory behind hierarchical fields is described in detail in Section III. The proposed tree-structured hierarchical field (TSHF) model is introduced in Section IV. The application of TSHF for SAR data and label-field synthesis is described in Section V. Synthesis results using operational RADARSAT-1 SAR sea-ice data provided by the Canadian Ice Service (CIS) and SIR-C/X-SAR land-mass data provided by the National Aeronautics and Space Administration Jet Propulsion Laboratory (NASA JPL) are presented and discussed in Section VI.

II. Related Work

While texture synthesis approaches for remote sensing data have been proposed in previous research literature [14]–[17], comparatively little attention has been paid to synthesizing remote sensing data with complex structural and textural characteristics. One can view the problem of generating structures for synthetic remote sensing data as a label-synthesis problem, where a label corresponds to a particular class of structure or feature (e.g., ice type, vegetation type).

While there is a large research literature [28], [29] on texture classification and processing, in most cases, the problem involves comparatively simple labels or lies at a single scale. In particular, many approaches utilize blob-like priors that enforce boundary smoothness and, as such, assert little in terms of subtle structures and complexity in the simulation of the field. Therefore, for synthesizing complex label fields, such as those in Fig. 1(c) and (d) illustrating structures in remote sensing imagery, a more subtle model is required.

The simplest method to improving the modeling of subtle structures is through the use of a Fourier basis for a Markov random field (MRF) model kernel [30], [31] method with threshold. Unfortunately, this approach is able to give only a stationary binary field and, even more problematic, only at a single scale. To capture complex scale structures, we have to get away from single-scale models such as local MRFs, two-point correlations [32], and local binary patterns [33].

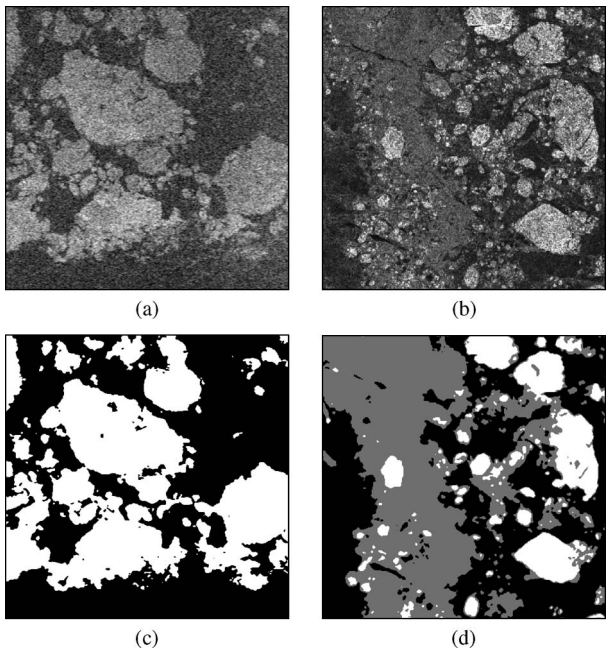

Fig. 1. [(a) and (b)] RADARSAT-1 SAR sea-ice texture samples and [(c) and (d) their underlying label maps]. Many SAR textures have underlying label maps with multiscale structures which can be (c) binary or (d) multilabeled. The scale-dependent behavior in (c) and (d) will usually not be well captured by a single random field.

Instead, hierarchical MRF modeling [34]–[36] provides a more natural and efficient way to deal with multiscale structures. However, the hierarchical models in [34]–[36] utilize simple models, like Ising or Potts at each scale, that are too limiting to capture complex structures. A different approach is the frozen-state hierarchical field (FSHF) model, which has been proposed for generating binary images with scale-dependent models and is computationally efficient [37]. Although it is possible to apply the FSHF to model a binary label map [Fig. 1(c)], this approach cannot be used directly in cases with more than two labels or with nonstationary behavior [Fig. 1(d)], both of which are common in remote sensing imagery.

Already discussed in the introduction is the significant literature on nonparametric texture synthesis methods [18]–[21]. These methods grow a synthesis by iteratively matching image patches in the synthesis and training. Being driven directly by the training data, these methods often produce good syntheses, but can miss large-scale or nonlocal phenomena, and suffer from patch copying when the patch size is set too large.

There is an established literature on the use of partition trees to decompose multilabel problems in image segmentation, compression, and synthesis [22]–[24], [38]. In this approach, a multilabel problem is repeatedly partitioned to yield a set of simple problems. In the past, the simple partitioned problem was solved using simple models, such as a single MRF. However, as we will see, a partitioned label field may still possess sufficiently complex scale-dependent structure to require a more sophisticated model, such as the FSHF.

III. Hierarchical Fields

In this paper, we are proposing to do data and label synthesis on the basis of first synthesizing the label field, specifically

by combining two existing methods—hierarchical models and partitioning methods.

There exist a variety of approaches to synthesize label fields and, in particular, we are using methods taken from MRFs which have been widely used in discrete field modeling [39], [40]. In modeling a given label field U, an MRF [28], [29] characterized by a *local* neighborhood $\mathcal{N}_s$

$$p(u_s|u_{S\setminus s}) = p\left(u_s|u_{\mathcal{N}_s}\right) \tag{1}$$

cannot assert the presence of structures on more than one scale, whereas learning a huge *nonlocal* model which can, in principle, learn such structures is a prohibitive approach. Instead, to model a label field U having multiscale structure, we would propose using scale-dependent modeling, such that U is defined via a sequence of fields $\{U_k, k \in K = (0, 1, \ldots, M)\}$, where $k = 0$ denotes the finest scale and $k = M$ the coarsest. At each scale k, U_k is defined on site space S_k and results from the downsampling of $U \equiv U_0$. A hierarchical Markov random field (HMRF) model can be written as

$$p(u_0, \cdots, u_M) = \left[\prod_{k=0}^{M-1} p(u_k|u_{k+1})\right] \cdot p(u_M). \tag{2}$$

The advantage of hierarchical modeling is that nonlocal large-scale features become local at a sufficiently coarse scale; therefore, at each scale, a single MRF can be used to capture the features local to that scale, inherently allowing for scale-dependent structures. We will define $u_{k,s}$ to be the label state at site s on scale k, with an associated local neighborhood $\mathcal{N}_{k,s}$ and parent $u_{k+1,\wp(s)}$ on the next coarser scale.

1) Frozen-State Hierarchy Model: In defining a hierarchical model, two issues need emphasizing: 1) the interscale context and 2) the computational complexity. To effectively model the spatial context, the interscale relationships are defined as a Markov chain in [36] with $p(u_k|u_{K\setminus k}) = p(u_k|u_{k+1})$, whereas the intrascale relationships are MRF $p(u_{k,s}|u_{k,S\setminus s}) = p(u_{k,s}|u_{k+1,\wp(s)}, u_{k,\mathcal{N}_s^k})$. This model has attractive elements but remains computationally expensive.

To improve computational efficiency, an FSHF model was presented in [37] to synthesize binary images. In that work, a given binary field $(u = u_0)$ can be represented by a hierarchical field $\{u_k\}$, where $u_k = \Downarrow_k (u_0)$ is a downsampled field. At coarse scales $(k > 0)$, u_k is defined with a ternary state $u_k(s) \in \{0, 1, 1/2\}$, where 0, 1 (black, white) are determined states, and 1/2 (gray) is undetermined. In terms of *modeling*, a fine to coarse representation can be derived as

$$u_{k,s} = \begin{cases} 1 & \text{if } u_{k-1,q} = 1, \quad \forall q \in \Re_{k-1}(s) \\ 0 & \text{if } u_{k-1,q} = 0, \quad \forall q \in \Re_{k-1}(s) \\ \frac{1}{2} & \text{otherwise} \end{cases} \tag{3}$$

where $\Re_{k-1}(s)$ is the set of sites in scale $k-1$ corresponding to the location s in scale k. Then, for *synthesis*, the key idea of the FSHF model is that, at each scale, only the sites which are undetermined need to be sampled, with those sites determined by the parent scale fixed (or frozen)

$$p(u_{k,s}|u_{k,S\setminus s}) = \begin{cases} \delta_{u_{k,s},u_{k+1,\wp(s)}} & \text{if } u_{k+1,\wp(s)} \in \{0,1\} \quad \longleftarrow \text{Frozen} \\ p\left(u_{k,s}|u_{k,\mathcal{N}_{k,s}}\right) & \text{if } u_{k+1,\wp(s)} = \frac{1}{2} \quad \longleftarrow \text{Sampled.} \end{cases} \tag{4}$$

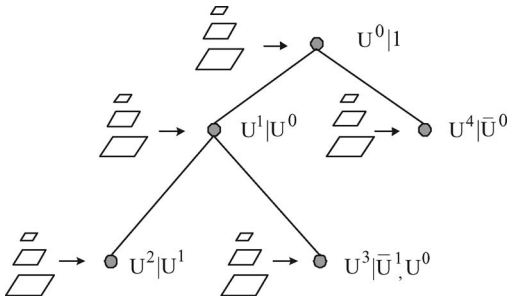

Fig. 2. Key concept of this paper: The modeling structure of TSHF. The partition tree has a hierarchical field at each node, where the field U_i is conditioned on the behavior of its parent, or both parent and grandparent.

With the frozen state, large scale features captured at the coarse scale are frozen and maintained to the fine scale, regardless of annealing schedule or sampling method. Since the interface between determined regions represents only a small fraction of most images, this approach offers a huge reduction in computational complexity relative to standard full-sampling hierarchical techniques. Given the significant computational benefits of the FSHF model, we are motivated to extend this modeling approach for the multistate case.

2) Multistate Hierarchy: In general, extending beyond binary modeling leads to rather complex representations and models, as well as to significant computational complexity. Although the FSHF model is effective in binary modeling, extending the method to multistate modeling is not a trivial step [27], [37]. The problem related to modeling all pairwise, triplet wise, etc., label interactions at coarser scales is quite complicated even for the ternary case.

However, for some ternary-state phenomena, if there is an intermediate medium acting as a physical separation or layer between two others, we have a particularly convenient context for modeling the ternary phenomenon. We can change the state definition of the FSHF by letting gray (1/2) denote the intermediate layer or undetermined, with the effect that the FSHF method can be directly applied and the intermediate state will lead to a ternary rather than binary field at the finest scale. We insist here on a spatial decoupling assumption that the intermediate state conditionally separates the other two states; in most cases, it will be simpler to decompose a complex multilabel structure into a set of simpler components as discussed in Section IV.

3) Modeling and Sampling: At each scale k, the FSHF can be formulated by a Gibbs distribution

$$p(u_k) = \frac{e^{-E_k(u_k)/T}}{\mathcal{Z}_k} \tag{5}$$

where T is a temperature, $\mathcal{Z}_k$ is the partition function, and $E_k(u_k)$ is the energy function at scale k.

A variety of energy functions [32] can be used to model complex structures. In the proposed modeling approach, we use a local histogram model [33], [41], a nonparametric model of all possible joint configurations within a 3×3 neighborhood with 2^9 binary or 3^9 ternary configurations. The energy function at each scale k is then defined as

$$E_k(u_k) = \sum_{n=0}^{N-1} \frac{\|h_k(u_k, n) - H_k(n)\|}{\nu_k(n) + \epsilon} \tag{6}$$

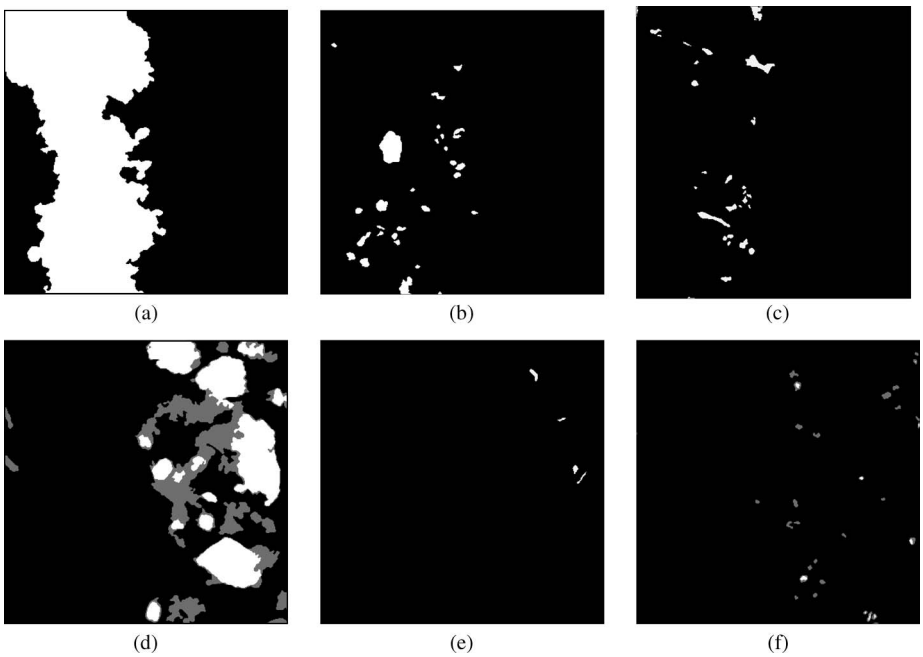

Fig. 3. Complex multilabel map can be decoupled as several binary or ternary fields with relatively simple structures. For example, the label map from Fig. 1(d) is decomposed here in (a)–(f). Although some fields, such as (a), (b), and (d), still contain structures at multiple scales, each decomposed field becomes much simpler than the original.

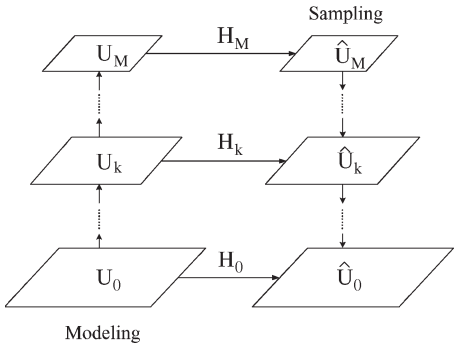

Fig. 4. Hierarchical modeling approach is a bottom–up process, starting at the finest scale to infer a different model at each scale. Hierarchical sampling, on the other hand, is a top-down process, starting at the coarsest scale then sampling at each scale k, constrained by the model H_k and parent state $\hat{U}_{k+1}$.

where N is the number of possible neighborhood configurations, H_k is the target histogram corresponding to the training data, h_k is the sample histogram corresponding to u_k, ν_k is a normalizing coefficient, and ϵ controls the penalty for unobserved $(H = 0)$ configurations.

In sampling, the FSHF algorithm is randomly initialized at the coarsest scale; the label field is then sampled by simulated annealing from coarse scale to fine scale. The hierarchical model and sampling scheme applied in this paper is shown in Fig. 4.

IV. TSHF

The FSHF method in Section III offers a compelling approach to modeling, which is computationally highly efficient, and admits a scale-dependent model for the synthesis of binary label maps. However, there are two obvious issues that need to be addressed for the synthesis of more complex label fields as encountered in remote sensing: First, we generally have to solve a multilabel problem; second, the label maps may be nonstationary, meaning that there are different behaviors in different parts of the image which cannot be well modeled by a single hierarchy. Forcing a single hierarchy to learn the variability of a nonstationary behavior leads to an averaging effect; thus, we need more than one model.

There is an existing literature on partition trees [22], [23] which allows a given image or label map to be partitioned into pieces. The general idea behind the partition tree is that behaviors are split and successively subdivided until homogeneous portions of images are found. In general, such binary partition trees can be used in problems of classification. Here, we choose to use them equally suitably in image synthesis as a proposed TSHF. The assumption is that a given multilabel image can be produced as a tree-structured conditional sequence of binary or ternary images, such that the dominant large-scale structure is produced first (the root node of the partition tree) and, then, with further details inside and outside of this structure, developed in the child nodes, a detailed example of which will be seen in the experimental results. The key idea is to use the existing method of partition trees to combine multiple hierarchical models to allow the nonstationary and nonbinary representation that we are seeking and at the same time to preserve the scale-dependent computational efficiency of the hierarchical approach. The modeling structure of TSHF is shown in Fig. 2.

In the proposed modeling approach, the structural components of U are progressively specified by a sequence of nodes in a binary tree $T = \{U^i | \mathcal{Q}^i, 0 \leq i < N\}$ from mixed to pure labeled states. Every node is defined as a conditional hierarchical field $U^i | \mathcal{Q}^i = \{U^i_k | \mathcal{Q}^i, k \in (0, 1, \ldots, M)\}$, where $\mathcal{Q}^i$ denotes the set of fields on which U^i depends. The partition

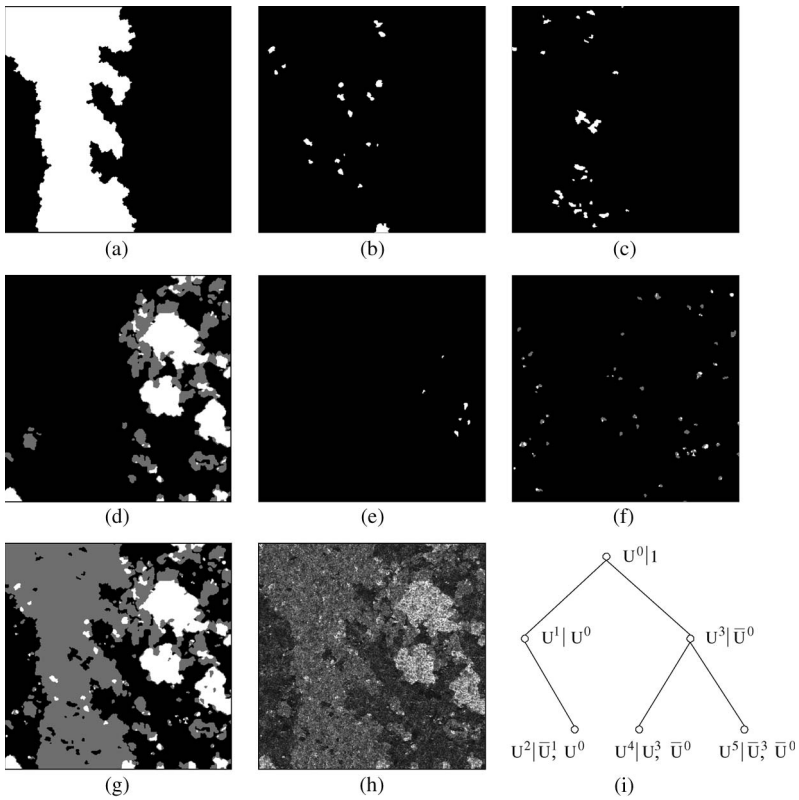

Fig. 5. Multilabel synthesis with the proposed tree-structured hierarchical model. [(a)–(f)] The synthesized component fields are shown, corresponding to the training samples shown in Fig. 3. The simple binary/ternary fields can be combined, based on (i) the tree structure, to achieve (g) the final label map, which is clearly similar to the true label map in Fig. 1(d). Given (g), (h) a synthesized sea-ice texture sample is produced. (a) $\hat{u}^0|1$. (b) $\hat{u}^1|\hat{u}^0$. (c) $\hat{u}^2|\hat{u}^0, \bar{\hat{u}}^1$. (d) $\hat{u}^3|\bar{\hat{u}}^0$. (e) $\hat{u}^4|\hat{u}^3, \bar{\hat{u}}^0$. (f) $\hat{u}^5|\bar{\hat{u}}^3, \bar{\hat{u}}^0$. (g) $\hat{u} = J(\hat{u}^0, \ldots, \hat{u}^5)$. (h) $\hat{x}$. (i) Partition tree.

tree starts at the root $U^0 = \{U_k^0 | \mathcal{Q}^0 = 1\}$, used to capture the most significant structure of U.

The influence of U^i on the partition tree is mediated through the up to two children of U^i, conditional on U^i or $\bar{U}^i$, such that binary field U^i controls the spatial extent of its children. The conditioning is encoded in $\mathcal{Q}^i$, which consists of one or more fields, such that

$$\begin{aligned} \mathcal{Q}^i = U^a \quad &\rightarrow \quad U_s^i = 0 \quad \text{if} \quad U_s^a = 0 \\ \mathcal{Q}^i = \bar{U}^a, U^b \quad &\rightarrow \quad U_s^i = 0 \quad \text{if} \quad U_s^a = 1 \text{ or } U_s^b = 0 \end{aligned} \tag{7}$$

etc.

Since each node under T only models simple binary/ternary structures, each field $U^i|\mathcal{Q}^i$ can be well modeled by the FSHF, as discussed in Section III, and each scale of each field $U_k^i|\mathcal{Q}^i$ can be sampled as

$$\hat{U}_k^i|\mathcal{Q}^i \leftarrow p\left(U_k^i|\mathcal{Q}^i|\hat{U}_{k+1}^i\right). \tag{8}$$

This process proceeds recursively, first over all scales in U^0 then over scales on fields further down the partition tree.

The process by which we infer a partition tree structure T from a given ground-truth label field $\overset{*}{u}$ is a creative one, requiring human input, and is highly problem dependent. The main example of this paper, the field shown in Fig. 1(d), has as its dominant large-scale structure the binary behavior $u^0|1$ [Fig. 3(a)]. Since both foreground and background in Fig. 3(a) correspond to mixed labels, the partition process needs to continue. The foreground is partitioned into two binary fields [Fig. 3(b) and (c)], whereas the background is decomposed into a Fig. 3(d) ternary field and Fig. 3(e) and (f) two minor residual binary ones. The original label field $\overset{*}{u}$ has thus been decomposed (Fig. 3), represented as a partition tree, as shown in Fig. 5(i).

Having specified a partition tree, the inverse step, the process of recombining the synthesized conditional fields $\{U^i|\mathcal{Q}^i\}$ to get $\hat{u} = J(\hat{u}^0, \ldots, \hat{u}^M)$ is straightforward.

Thus, the proposed TSHF method synthesizes a label field in two ways: In terms of shape complexity, the structure is gradually refined hierarchically from coarse to fine resolution; in terms of label complexity, the states are specified through a partition tree from coarse to fine labeling. The proposed modeling approach, with both resolution-oriented and region-oriented hierarchies, provides a capability to model complex discrete fields using simple models while maintaining high computational efficiency. A hierarchical model on its own, such as the FSHF, can be considered as a special case of the TSHF with only one region-oriented component.

Admittedly, one of the limitations of the proposed approach is its spatial decoupling assumption, which assumes that a multilabel field can be decomposed into multiple binary/ternary fields. In some cases, in which the different label regions are highly interacting, this assumption may not hold true; however, our tests show that a variety of SAR and other data can indeed be modeled in this way.

The overall modeling process (Algorithm I) is therefore to select a partition tree to find the ground truth for each state

in the partition and to learn a histogram model H_k^i in (6) from the empirical histogram of the ground-truth data for each scale k in model i. With the modeling performed, the sampling process follows the dependency structure of the partition tree. Each hierarchy is randomly initialized at the coarsest scale and sampled at progressively finer scales using simulated annealing. When all of the frozen state hierarchies have been sampled, the generated fields are combined according to the partition-tree structure to obtain the label synthesis.

Algorithm I: TSHF Modeling

1) Initialize a training partition tree $T = \{U^i | \mathcal{Q}^i, 0 \leq i < N\}$.
2) Learn a hierarchical histogram model H_k^i at k scales for each conditional node $U^i|\mathcal{Q}^i$ in T.
3) Initialize each sampling hierarchy randomly at the coarsest scale.
4) Sample each hierarchical model from coarser to finer scales by using simulated annealing.
5) Combine the generated fields to the partition-tree structure and obtain the synthesized label field.

V. Image Synthesis

The textured data in Fig. 1(a) and (b), having a complex nonlocal nonstationary behavior, are difficult to model. Therefore, the direct synthesis

$$\hat{x} \leftarrow p(x) \tag{9}$$

is a complicated undertaking. On the other hand, because U represents the salient features of interest in X, what remains in X, given U, are the fine-scale details not of interest, namely, noise, speckle, quantization, blurring, etc.; all of which are comparatively simple and *local* textural phenomena. That is, the synthesis

$$\hat{x} \leftarrow p(x|\hat{u}) \tag{10}$$

is comparatively straightforward; therefore, we are deliberately picking an existing texture synthesized method [18] to generate the fine-scale texture on top of $\hat{u}$.

The method in [18] is a sample-based approach to synthesis, such that a pixel x_s is synthesized by comparing its neighborhood X_{N_s} to all possible neighborhoods in the training data $\overset{*}{x}$ and selecting x_s at random from among the matching $\overset{*}{x}$ neighborhoods.

We slightly modify the method of [18] to allow a synthesized texture $\hat{x}$ to be sampled from the conditional MRF $X|U$

$$\hat{x}_s \leftarrow p\left(x_s | x_{\mathcal{N}_s}, u_s\right) \tag{11}$$

rather than directly from the texture field X. Given the conditioning on u_s, we now search for a set of closely matching patches in $\overset{*}{x}$, for which the training label $\overset{*}{u}$ also matches.

We will see in Section VI that this simple texture synthesis approach leads to good results. There is nothing inherent necessitating the use of [18] with our approach; indeed, any other advanced texture synthesis method may be used as well.

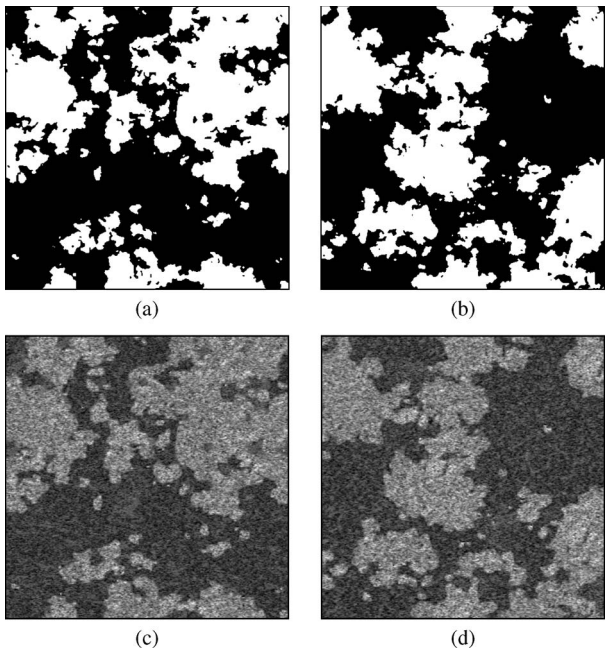

Fig. 6. Binary-label sea-ice samples synthesized using a frozen-state hierarchical model. Trained by the label sample in Fig. 1(c), [(a) and (b)] the synthesized label maps not only maintain similar format structure statistics of the training sample but also have significant variations. Conditioned on (a) and (b), it is straightforward to sample the textures shown in (c) and (d), comparable to the true sea-ice sample of Fig. 1(a).

VI. Experimental Results

This paper proposes two goals:

1) the synthesis of realistic SAR data;
2) the synthesis of the underlying label field as ground truth.

To demonstrate the effectiveness of the proposed TSHF model, the data synthesis approach described in Sections IV and V was used to generate random SAR sea-ice data based on operational RADARSAT-1 SAR sea-ice data of the polar region provided by the CIS, as well as SIR-C/X-SAR land-mass data of Hong Kong, China, provided by NASA JPL. The SAR sea-ice data used to learn the model for generating sea-ice imagery are acquired in the microwave band (C-band), with HH polarization, 100-m pixel spacing, and three ice types. The sea-ice data of the polar region are difficult to model and synthesize given the complex sea-ice structures and formations, as well as nonhomogeneous texture characteristics. The SAR land-mass data of Hong Kong, China, used to learn the model for generating land-mass imagery are acquired in the microwave band (C-band). The sea-ice and land-mass data are very different from one another, with the intent of illustrating that our method is not specialized to a single type of SAR data.

A. Single Hierarchical Approach

A single hierarchical field model, such as the FSHF, can be considered as a special case of the TSHF with only one component. As the first test for the proposed model, we apply a single FSHF model to synthesize a scale-dependent binary field. This initial test is undertaken to demonstrate the morphological modeling performance of a single hierarchy in modeling a binary field. The model is trained by the binary field $\overset{*}{u}$ shown in Fig. 1(c). Two synthesized samples $\hat{u}$ are shown in Fig. 6(a)

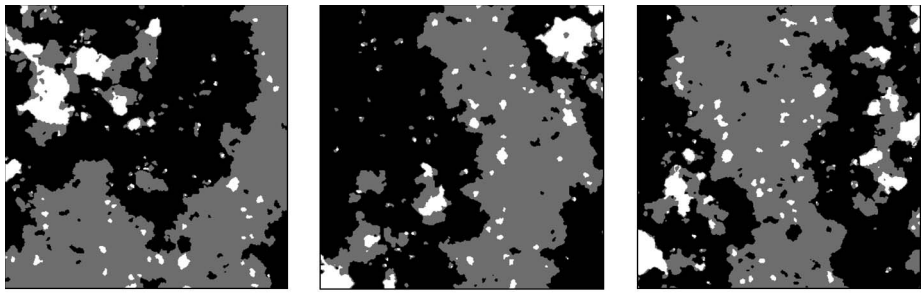

(a) (b) (c)

Fig. 7. Multilabel sea-ice samples synthesized with multiple runs based on the same training samples from Fig. 3 and the same tree structure in Fig. 5(i).

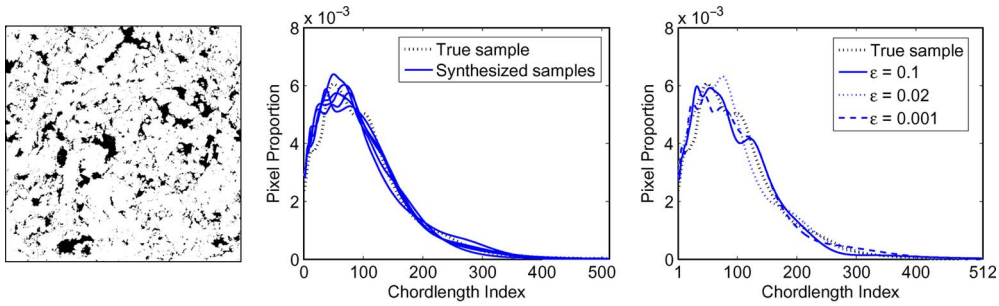

(a) (b) (c)

Fig. 8. Hierarchical model of the proposed modeling structure is evaluated using a chordlength model [42]. (a) Large binary microscopic excerpt (2048 × 2048) for model evaluation. (b) Chordlength distributions from multiple synthesis runs. (c) Chordlength as a function of parameter ϵ in (6).

and (b). We can see that the structures in the synthesized fields essentially resemble the multiscale phenomena of the training data.

The texture at each pixel $\hat{x}_s$ is sampled, as described in Section V. In the synthesized texture samples, Fig. 6(c) and (d), we see that the created texture skin is consistent with the texture characteristics in the training data shown in Fig. 1(a).

B. Tree-Structured Hierarchical Approach

A more general test for the proposed TSHF is the image shown in Fig. 1(b), with a corresponding label field in Fig. 1(d). Based on the tree-structured modeling representation of Section IV, a partition tree of binary or ternary component fields $\overset{*}{u}^{i}$ is constructed, as shown in Fig. 5(i), such that the hidden field is produced from the components as

$$\begin{aligned}\hat{u} &= J(\hat{u}^0, \cdots, \hat{u}^M) \\ &= \hat{u}^0 | 1 + \hat{u}^1 | \hat{u}^0 - \hat{u}^2 | \hat{u}^0, \bar{\hat{u}}^1 + \hat{u}^3 | \bar{\hat{u}}^0 - \hat{u}^4 | \hat{u}^3, \bar{\hat{u}}^0 \\ &\quad + \hat{u}^5 | \bar{\hat{u}}^3, \bar{\hat{u}}^0 \end{aligned} \tag{12}$$

where the partition tree structure is subjectively inferred, by hand, from the training data.

We thus obtain a complex synthesized multilabel field [Fig. 5(g)]. By comparing Fig. 5(a)–(f) to Fig. 3(a)–(f), respectively, we can see that the synthesized components generally resemble the multiscale structure in their corresponding training components. Since the structured features of each training component can be well captured by each node hierarchy, the final label field should possess similar statistical characteristics to the training data, comparing Fig. 5(g) to Fig. 1(d). Given the synthesized label field [Fig. 5(g)], the sea-ice texture may be generated [Fig. 5(h)] and can be compared with Fig. 1(b).

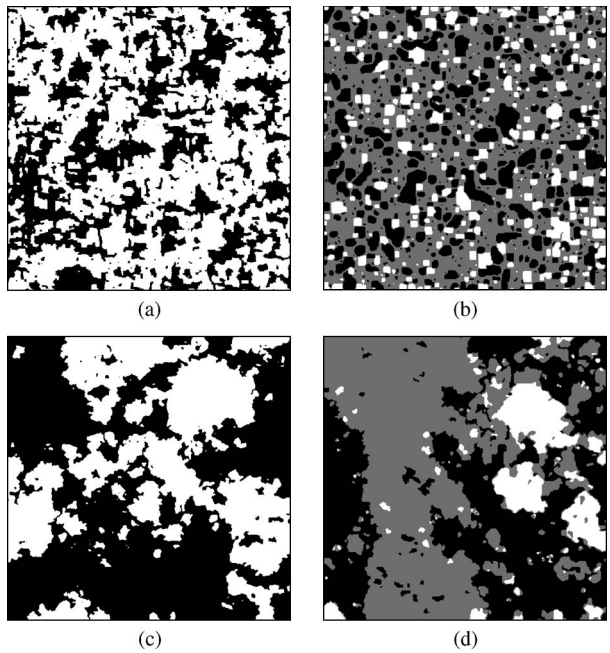

(a) (b) (c) (d)

Fig. 9. Sea-ice label map synthesis comparison. Panels (a) and (b) show the label fields resulting from single Markov fields based on chordlength and local-histogram models, whereas panels (c) and (d) show the label fields from the scale-dependent FSHF and TSHF, respectively. It is clear that the single Markov models can only provide stationary fields, with structure on one scale, as opposed to the nonstationary and scale-dependent structures possessed by the real label maps in Fig. 1(c) and (d), which are well captured by the multiscale models in the FSHF and the TSHF. (a) Two-phase black/white chordlength model [42]. (b) Local histogram model [41]. (c) FSHF. (d) Proposed TSHF.

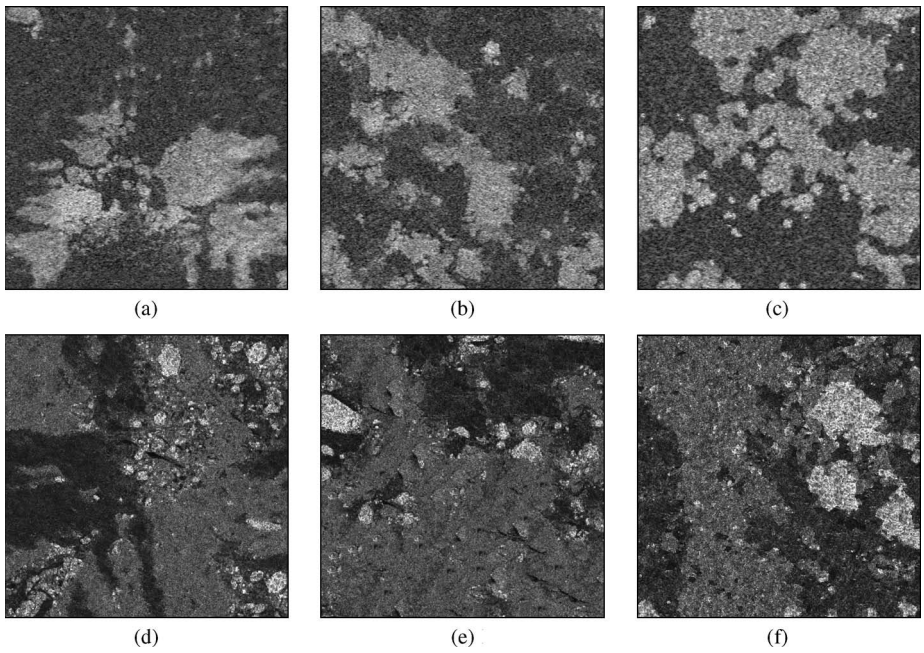

Fig. 10. Sea-ice texture synthesis comparison, based on [(a) and (d)] the pixel-based nonparametric sampling method [18], [(b) and (e)] patch-based sampling method [19], and our [(c) and (f)] texture synthesis method proposed in Section V. The top row shows two-label synthesis results and should be compared to Fig. 1(a). The bottom row shows three-label syntheses compared to Fig. 1(b). The difficulty in producing large-scale structure is particularly apparent in the [(d) and (e)] three-label case relative to (f) our result.

To emphasize the variability in the synthesized samples and the suitability of our approach in generating ground-truth test data, three additional results based on the same training data are shown in Fig. 7. We can see that the synthesized label fields provide substantial variations and yet share similar statistical characteristics.

The hierarchical model in the proposed modeling structure is evaluated, as plotted in Fig. 8, using a chordlength model [42] from a large (2048×2048) binary sample [Fig. 8(a)]. This test sample, a microscopic image of a physical porous medium, contains a wide variety of multiscale structures, exactly the sort of structure our proposed hierarchical model is expected to model. Comparing the chordlength plots between the synthesized and true fields [Fig. 8(b)], the chordlength model, which is unrelated to our model in (6), validates the consistency of the synthesized samples with each other and with the true sample. The sensitivity of the free parameter ϵ in (6) is assessed by generating samples as a function of ϵ; as shown in Fig. 8(c), the proposed algorithm is insensitive to small ϵ.

To illustrate the strength of the TSHF, we compare our proposed method with other methods in label field modeling and texture synthesis. First, a single MRF is used to synthesize both binary and ternary fields based on Fig. 1(c) and (d). The synthesized label fields are shown in Fig. 9(a) and (b) where we see that the synthesized structures are local and stationary, rather than presenting the multiscale structures appearing in the true label maps. In contrast, the FSHF and TSHF models exhibit their capabilities of capturing complex structures in the label fields by capturing the presence of scale-dependent behavior in Fig. 9(c) and (d).

As a second comparison, we compare our proposed data synthesis method with two nonparametric texture synthesis methods: one is a pixel-based sampling [18] and the other is a patch-based sampling [19]. The basic idea of both nonparametric methods is to directly sample the given image by using self-similarity, a concept widely used in texture synthesis. For the relatively simple sea-ice training data in Fig. 1(a), the generated textures from the two comparison methods are given in Fig. 10(a) and (b), which provide a good reproduction of the training sample. Similarly, given the training data with more complex structure in Fig. 1(b), the nonparametric methods also provide quite attractive results in Fig. 10(d) and (e) and demonstrate a good ability in structure representation.

However, there are three significant issues. First, the nonparametric methods are sensitive to the synthesis staring seed, such that for certain seeds the synthesis may fail to sense certain significant structures present in the training data, as may be seen in comparing Fig. 10(e) with Fig. 1(b). Second, the nonparametric methods are sensitive to window size, such that a small window fails to sense large-scale structure, whereas a large window can lead to copying portions of the training image, as may be seen in Fig. 10(d), rather than random sampling. Finally, and most significantly, the texture synthesis methods synthesize *only* the texture and have no notion of the underlying label field, which is essential for the testing of classification and segmentation algorithms.

A third experiment compares to a recent method [21] in which a nonparametric method *does* generate the label field as part of synthesis. Developed from the patch-based sampling method of [19], the method inherits the same advantages and disadvantages of patch-based methods. Because the focus of [21] was on texture synthesis, and not necessarily the quality of the underlying field, the synthesized ground truth is relatively poor, as shown in Fig. 11. In particular, the synthesized label field is rather sensitive patch size [Fig. 11(a)–(c)] and suffers from blocky and repetitive artifacts [Fig. 11(c), (d), and (f)].

As a final experiment, in contrast to the sea-ice imagery shown in the previous examples, land-mass imagery in

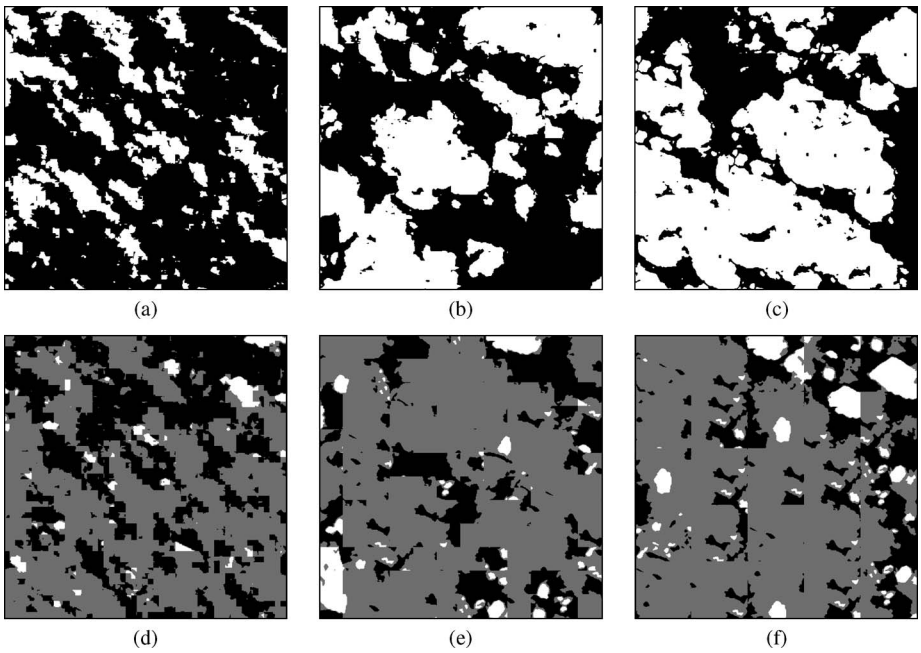

Fig. 11. Sea-ice label map synthesized by the IceSynth2 method [21]. Based on the binary and ternary label samples of Fig. 1(c) and (d), samples (a)–(c) and (d)–(f) are synthesized with the stated patch sizes. The sensitivity of the result to patch size is clear, as is the blockiness and repetitive artifacts in (c), (d), and (f). (a) Block size 10×10. (b) Block size 40×40. (c) Block size 100×100. (d) Block size 10×10. (e) Block size 40×40. (f) Block size 100×100.

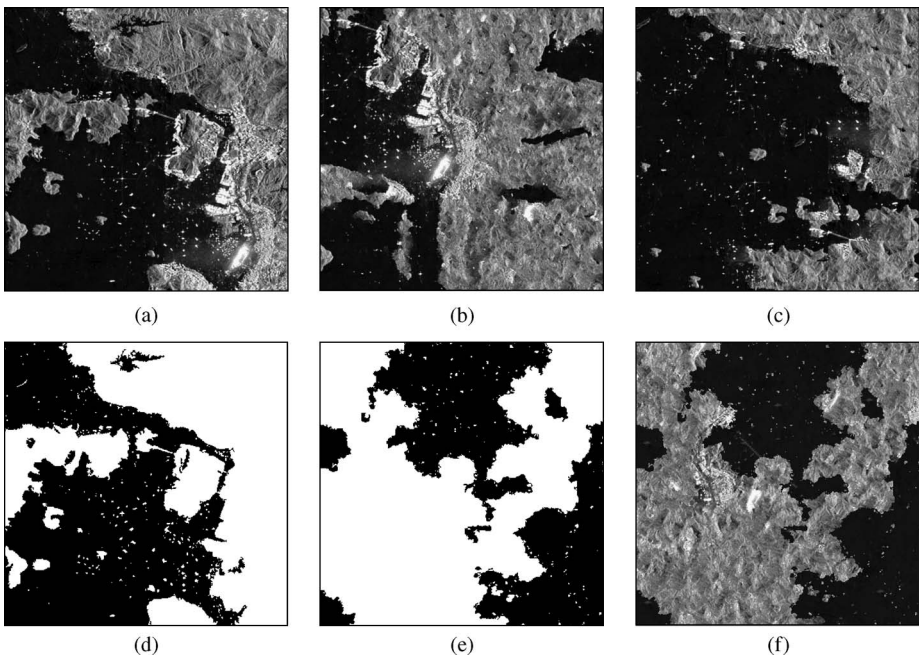

Fig. 12. (a) SIR-C/X-SAR land-mass imagery with (d) its given label field. Both (e) the synthesized label field and (f) texture resemble (d) the true label map and (a) texture well. (a) Land-mass image. (b) Method of [18]. (c) Method of [19]. (d) True label field of (a). (e) Synthesized label field from the proposed TSHF. (f) Synthesized texture from (e).

Fig. 12(a), with a corresponding label field in Fig. 12(d), is also used as training samples. The synthesized label field and texture are shown in Fig. 12(e) and (f). Compared to the results in Fig. 12(b) and (c), from the nonparametric methods [18], [19], our proposed approach shows more flexibility in producing random syntheses, particularly, given the similar structures which appear in the nonparametric syntheses, copied from the training data.

VII. Conclusion

In this paper, a novel modeling approach has been introduced for capturing complex nonstationary scale-dependent structures in complex SAR data. The proposed TSHF model integrated a region-oriented binary tree structure with a resolution-oriented hierarchical approach to allow for complex multiscale structure modeling while maintaining high computational efficiency. The application of the proposed model for synthesizing complex

SAR data with complex multiscale structural characteristics has been presented, and experimental results using operational RADARSAT-1 SAR sea-ice and SIR-C/X-SAR land-mass data have demonstrated the effectiveness of the proposed model at producing realistic synthesized SAR data and corresponding ground-truth label fields. Although, here, the proposed approach has been demonstrated in the synthesis of SAR sea-ice and land-mass data, it is nonspecific and can be applied to a wide variety of different remote sensing problems. The primary limitations of the proposed approach are the need for a manual partition tree and the strict spatial decoupling assumption; both limitations are the subject of ongoing work.

ACKNOWLEDGMENT

The authors would like to thank the Canadian Ice Service and Prof. D. A. Clausi, Department of Systems Design Engineering, University of Waterloo, for providing the sea-ice data, the National Aeronautics and Space Administration Jet Propulsion Laboratory for providing the land-mass data, and the Natural Sciences and Engineering Research Council of Canada for supporting this research.

REFERENCES

[1] Q. Yu and D. Clausi, "SAR sea-ice image analysis based on iterative region growing using semantics," *IEEE Trans. Geosci. Remote Sens.*, vol. 45, no. 12, pp. 3919–3931, Dec. 2007.

[2] L. Kiage, K. Liu, N. Walker, N. Lam, and O. Huh, "Recent land-cover/use change associated with land degradation in the Lake Baringo catchment, Kenya, East Africa: Evidence from landsat TM and ETM+," *Int. J. Remote Sens.*, vol. 28, no. 19, pp. 4285–4309, Jan. 2007.

[3] T. Landmann, C. Herty, S. Dech, and M. Schmidt, "Land cover change analysis within the GLOWA Volta basin in West Africa using 30-meter landsat data snapshots," in *Proc. IEEE Int. Geosci. Remote Sens. Symp.*, 2007, pp. 5298–5301.

[4] C. V. der Sande, S. de Jong, and A. de Roo, "A segmentation and classification approach of IKONOS-2 imagery for land cover mapping to assist flood risk and flood damage assessment," *Int. J. Appl. Earth Observ. Geoinform.*, vol. 4, no. 3, pp. 217–229, Jun. 2003.

[5] R. Samadani, "A finite mixture algorithm for finding proportions in SAR images," *IEEE Trans. Image Process.*, vol. 4, no. 8, pp. 1182–1186, Aug. 1995.

[6] Q. Redmund, D. Long, and M. Drinkwater, "Polar sea-ice classification using enhanced resolution NSCAT data," in *Proc. IEEE Int. Geosci. Remote Sens. Symp.*, 1998, vol. 4, pp. 1976–1978.

[7] J. Karvonen, "Baltic sea ice SAR segmentation and classification using modified pulse-coupled neural networks," *IEEE Trans. Geosci. Remote Sens.*, vol. 42, no. 7, pp. 1566–1574, Jul. 2004.

[8] L. Soh, C. Tsatsoulis, D. Gineris, and C. Bertoia, "Arktos: An intelligent system for SAR sea ice image classification," *IEEE Trans. Geosci. Remote Sens.*, vol. 42, no. 1, pp. 229–248, Jan. 2004.

[9] R. Kettig and D. Landgrebe, "Classification of multispectral images by extraction and classification of homogeneous objects," *IEEE Trans. Geosci. Remote Sens.*, vol. 14, pp. 19–26, Jan. 1976.

[10] F. Melgani and L. Bruzzone, "Classification of hyperspectral remote sensing images with support vector machines," *IEEE Trans. Geosci. Remote Sens.*, vol. 42, no. 8, pp. 1778–1790, Aug. 2004.

[11] J. Benediktsson, M. Pesaresi, and K. Amason, "Classification and feature extraction for remote sensing images from urban areas based on morphological transformations," *IEEE Trans. Geosci. Remote Sens.*, vol. 41, no. 9, pp. 1940–1949, Sep. 2003.

[12] M. Pesaresi and J. Benediktsson, "A new approach for the morphological segmentation of high-resolution satellite imagery," *IEEE Trans. Geosci. Remote Sens.*, vol. 39, no. 2, pp. 309–320, Feb. 2001.

[13] G. Meinel and M. Neubert, "A comparison of segmentation programs for high resolution remote sensing data," *Int. Arch. ISPRS*, vol. 35, pp. 1097–1105, 2004.

[14] D. Blacknell, A. Blake, P. Lombardo, and C. Oliver, "A comparison of simulation techniques for correlated gamma and K-distributed images for SAR applications," in *Proc. IEEE Int. Geosci. Remote Sens. Symp.*, 1994, vol. 4, pp. 2182–2184.

[15] D. Blacknell, "A new method for the simulation of K-distribution clutter," *Proc. Inst. Elect. Eng.—Radar Sonar Navig.*, vol. 141, no. 1, pp. 53–58, Feb. 1994.

[16] H. Cantalloube, "Texture synthesis for SAR image simulation," *Proc. SPIE*, vol. 3497, pp. 242–250, 1998.

[17] Y. Wu, C. Wang, H. Zhang, X. Wen, and B. Zhang, "Statistical analysis and simulation of high-resolution SAR ground clutter data," in *Proc. IEEE Int. Geosci. Remote Sens. Symp.*, 2008, vol. 4, pp. 2182–2184.

[18] A. A. Efros and T. K. Leung, "Texture synthesis by non-parametric sampling," in *Proc. IEEE ICCV*, 1999, pp. 1033–1038.

[19] L. Liang, C. Liu, Y. Xu, B. Guo, and H. Shum, "Real-time texture synthesis by patch-based sampling," *ACM Trans. Graph.*, vol. 20, no. 3, pp. 127–150, Jul. 2001.

[20] L. Wei and M. Levoy, "Fast texture synthesis using tree-structured vector quantization," in *Proc. 27th Annu. Conf. Comp. Graph. Interactive Techn.*, 2000, pp. 479–488.

[21] A. Wong, P. Yu, W. Zhang, and D. Clausi, "Icesynth II: Synthesis of sar sea-ice imagery using region-based local conditional posterior sampling," *IEEE Geosci. Remote Sens. Lett.*, vol. 7, no. 2, pp. 348–351, Apr. 2009.

[22] P. Salembier and L. Garrido, "Binary partition tree as an efficient representation for image processing, segmentation, and information retrieval," *IEEE Trans. Image Process.*, vol. 9, no. 4, pp. 561–576, Apr. 2000.

[23] C. D'Elia, G. Poggi, and G. Scarpa, "A tree-structured Markov random field model for Bayesian image segmentation," *IEEE Trans. Image Process.*, vol. 12, no. 10, pp. 1259–1273, Oct. 2003.

[24] G. Poggi, G. Scarpa, and J. B. Zerubia, "Supervised segmentation of remote sensing images based on a tree-structured MRF model," *IEEE Trans. Geosci. Remote Sens.*, vol. 43, no. 8, pp. 1901–1911, Aug. 2005.

[25] G. Scarpa, R. Gaetano, M. Haindl, and J. Zerubia, "Hierarchical multiple Markov chain model for unsupervised texture segmentation," *IEEE Trans. Image Process.*, vol. 18, no. 8, pp. 1830–1843, Aug. 2009.

[26] R. Gaetano, G. Scarpa, and G. Poggi, "Hierarchical texture-based segmentation of multiresolution remote-sensing images," *IEEE Trans. Geosci. Remote Sens.*, vol. 47, no. 7, pp. 2129–2141, Jul. 2009.

[27] Y. Liu and P. Fieguth, "Parallel hidden hierarchical fields for multi-scale reconstruction," in *Proc. EMMCVPR*, *LNCS*, Aug. 2009, pp. 70–83.

[28] S. Geman and D. Geman, "Stochastic relaxation, gibbs distributions, and the bayesian restoration of images," *IEEE Trans. Pattern Anal. Mach. Intell.*, vol. PAMI-6, no. 6, pp. 721–741, Nov. 1984.

[29] R. Chellappa, "Two-dimensional discrete Gaussian Markov random field models for image processing," in *Progress in Pattern Recognition*, vol. 2, L. N. Kanal and A. Rosenfeld, Eds. New York: Springer-Verlag, 1985, pp. 79–112.

[30] P. Davis, *Circulant Matrices*. New York: Wiley-Interscience, 1979.

[31] H. Rue and L. Held, *Gaussian Markov Random Field: Theory and Applications*. Boca Raton, FL: CRC Press, 2005.

[32] S. Torquato, *Random Heterogeneous Materials: Microstructure and Macroscopic Properties*. New York: Springer-Verlag, 2002.

[33] T. Ojala, M. Pietikainen, and D. Harwood, "A comparative study of texture measures with classification based on feature distributions," *Pattern Recognit.*, vol. 29, no. 1, pp. 51–59, Jan. 1996.

[34] C. Graffigne, F. Heitz, P. Pérez, F. Prêux, M. Sigelle, and J. Zerubia, "Hierchical Markov random field models applied to image analysis: A review," *Proc. SPIE*, vol. 2568, pp. 2–17, Aug. 1994.

[35] Z. Kato, M. Berthod, and J. Zerubia, "A hierarchical Markov random field model and multitemperature annealing for parallel image classificaion," *Graph. Models Image Process.*, vol. 58, no. 1, pp. 18–37, Jan. 1996.

[36] M. Mignotte, C. Collet, P. Pérez, and P. Bouthemy, "Sonar image segmentation using an unsupervised hierarchical MRF model," *IEEE Trans. Image Process.*, vol. 9, no. 7, pp. 1216–1231, Jul. 2000.

[37] W. Campaigne, P. Fieguth, and S. Alexander, "Frozen-state hierarchical annealing," in *Proc. ICIAR*, *LNCS*, 2006, pp. 41–52.

[38] C. B. Atkins, C. A. Bouman, and J. P. Allebach, "Tree-based resolution synthesis," in *Proc. Image Process. Image Qual., Image Capture Syst. Conf.*, 1999, pp. 405–410.

[39] C. Won and R. Gray, *Stochastic Image Processing*. New York: Plenum, 2004.

[40] S. Z. Li, *Markov Random Field Modeling in Computer Vision*. New York: Springer-Verlag, 1995.

[41] S. K. Alexander, P. Fieguth, M. Ioannidis, and E. R. Vrscay, "Hierarchical annealing for synthesis of binary porous media images," *Math. Geosci.*, vol. 41, no. 4, pp. 357–378, May 2009.

[42] M. Talukdar, O. Torsaeter, and M. Ioannidis, "Stochastic reconstruction of particulate media from two-dimensional images," *J. Colloid Interface Sci.*, vol. 248, no. 2, pp. 419–428, Apr. 2002.

Ying Liu (S'07) received the B.Eng. degree from the Huazhong University of Science and Technology, Wuhan, China, in 1999 and the M.Sc. degree from the Chinese Academy of Sciences, Beijing, China, in 2002. She is currently working toward the Ph.D. degree in systems design engineering at the University of Waterloo, Waterloo, ON, Canada.

She was with the Institute of Acoustics, Chinese Academy of Sciences, from 2002 to 2006. Her current research interests include image processing, analysis, and modeling, and image and video coding.

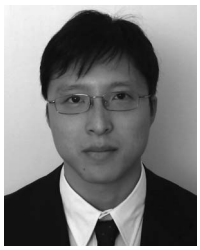

Alexander Wong (M'05) received the B.A.Sc. degree in computer engineering, the M.A.Sc. degree in electrical and computer engineering, and the Ph.D. degree in systems design engineering from the University of Waterloo, Waterloo, ON, Canada, in 2005, 2007, and 2010, respectively.

He is currently with the Department of Systems Design Engineering, University of Waterloo. He has authored or coauthored papers in various fields such as computer vision, graphics, image processing, biomedical signal processing, remote sensing, and multimedia systems, published in refereed journals and conferences. His current research interests include remote sensing and biomedical image processing and analysis, computer vision, and pattern recognition. He has been involved in projects on image registration, image denoising, image superresolution, image segmentation, video tracking, remote sensing and biomedical image analysis, and image and video coding.

Paul Fieguth (S'87–M'96) received the B.A.Sc. degree in electrical engineering from the University of Waterloo, Waterloo, ON, Canada, in 1991 and the Ph.D. degree in electrical engineering from the Massachusetts Institute of Technology (MIT), Cambridge, in 1995.

He joined the faculty at the University of Waterloo, in 1996, where he is currently an Associate Professor in systems design engineering. He has held visiting appointments at the Cambridge Research Laboratory, Oxford University, Oxford, U.K., Rutherford Appleton Laboratory, Chilton, U.K., and the Institut national de recherche en informatique et en automatique/Sophia-Antipolis, France, with postdoctoral positions in computer science at the University of Toronto, Toronto, ON, and in information and decision systems at MIT. His research interests include statistical signal and image processing, hierarchical algorithms, data fusion, and the interdisciplinary applications of such methods, particularly to remote sensing.